Chapter IV

EXPERIMENTAL RESULTS

4.1 Determination of Shape Factor and Density of Oil Shale Particles

Table 4.1 shows the relation of the nitrogen velocity (U_o) and the derived formula of $(\frac{980}{180} \cdot \frac{\Delta P}{L_m} \cdot \frac{\bar{d}_p^2}{\mu})$. K_i was obtained by plotting, as shown in Fig. 4.1.

These K_i values of 1.140, 1.049 and 0.986 were calculated in terms of $(1/K_i L_m^2)^{1/3}$ as tabulated in Table 4.2. Then $(1/K_i L_m^2)^{1/3}$ was plotted against the reciprocal of the height of bed $(\frac{1}{L_m})$, as shown in Fig. 4.2. From the curve, intercept a and slope b values are 0.45 and 0.90, respectively. The results led to the determination of the shape factor and density of oil shale particles as follows :

From Eq. 3.6, $\phi = a^{\frac{1}{2}} b$

$= (0.45)^{\frac{1}{2}} \cdot 0.90 = 0.604$

and from Eq. 3.7, $\rho_s = \frac{a}{b} \cdot \frac{W}{S}$

$= \frac{0.45}{0.90} \cdot \frac{100}{20.276} = 2.47 \text{ gm/cm}^3$

Table 4.1 The Relationship between U_o and $(\frac{980}{180} \cdot \frac{\Delta P}{L_m} \cdot \frac{\bar{d}_p^2}{\mu})$ in Determining K_i

W = 100.00 gm.

$\bar{d}$ = 0.031 cm. (Appendix B.1)

μ = 1.76×10^{-4} poise at 30°C From Perry et al (23)

S = 20.276 cm^2.

Run No.	U_o (cm/sec)	ΔP (gm/cm^2)	L_m (cm)	$\frac{980}{180} \cdot \frac{\Delta P}{L_m} \cdot \frac{\bar{d}_p^2}{\mu}$
1	8.23	1.74	5.70	9.07
	6.08	1.31		6.83
	3.93	0.84		4.38
	1.87	0.41		2.14
2	8.23	1.60	5.85	8.13
	6.08	1.20		6.10
	3.93	0.78		3.96
	1.87	0.39		1.98
3	8.23	1.51	5.95	7.54
	6.08	1.12		5.60
	3.93	0.73		3.65
	1.87	0.37		1.85

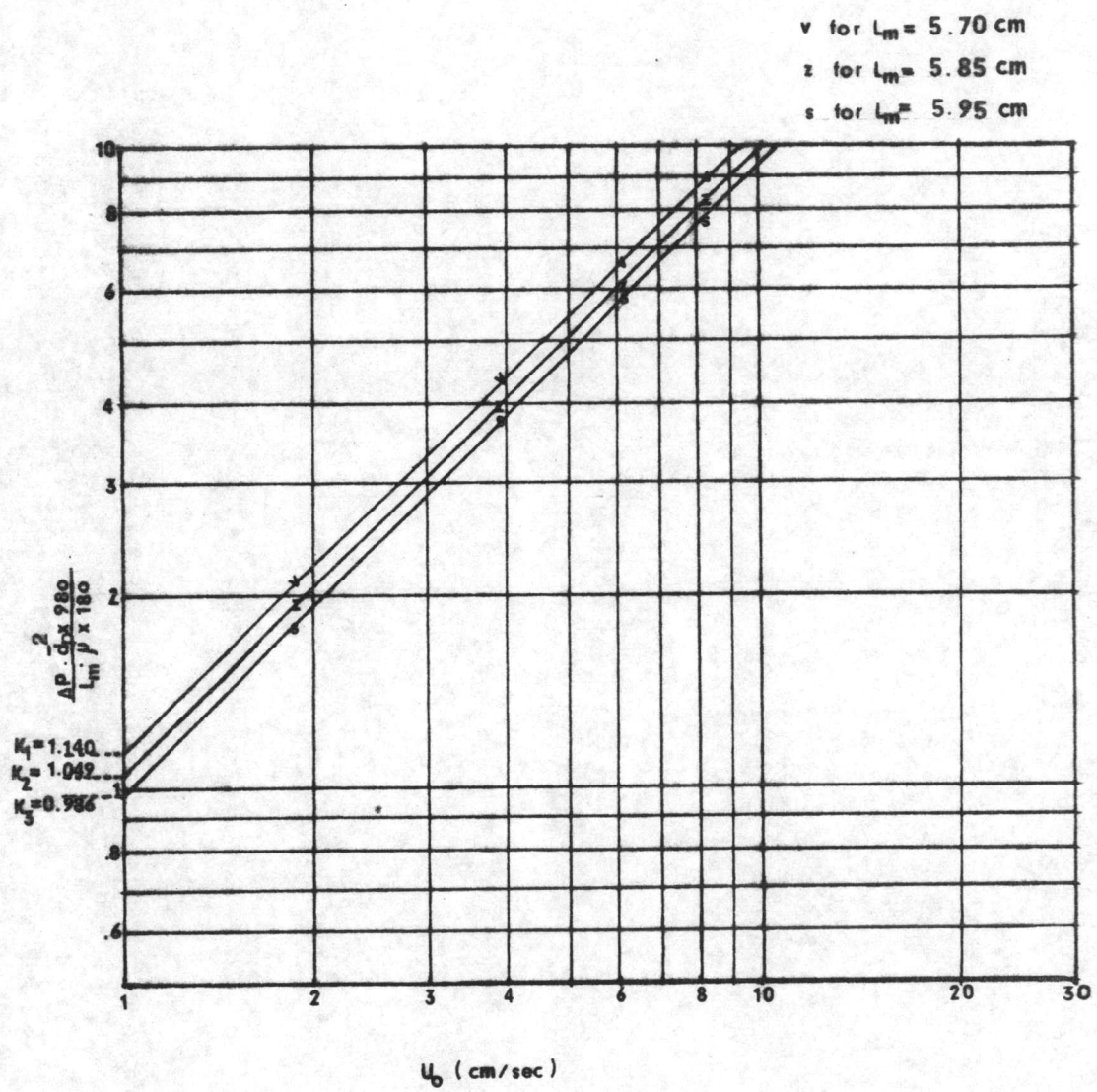

FIG. 4.1— DETERMINATION OF K_1 IN EQ.(3-4) FROM TABLE 4.1

Table 4.2 The Relationship between K_i and L_m in Determining ϕ and ρ_s

Run No.	K_i	L_m (cm)	$(1/K_i L_m^2)^{1/3}$	$\frac{1}{L_m}$
1	1.140	5.70	0.300	0.175
2	1.049	5.85	0.304	0.171
3	0.986	5.95	0.306	0.168

The bulk density of oil shale as experimented by water displacement method (10) was 2.30 gm/cm^3, which is close to the density of oil shale particles. This indicates that shale particle size has small effect on its density.

The values of the shape factor and oil shale particle density then were used in retort design (Appendix A).

4.2 Determination of the Actual Minimum Fluidizing Velocity.

Table 4.3 shows the data of the actual minumum fluidizing velocity in raw shale bed. The mean particle sizes of 0.715, 0.576, and 0.249 mm were referred to as sample 1, 2, and 3, respectively (Appendix B.1). When the pressure drop was plotted against the nitrogen velocity in the log-log paper, the actual minimum fluidizing velocity of sample 1, 2,

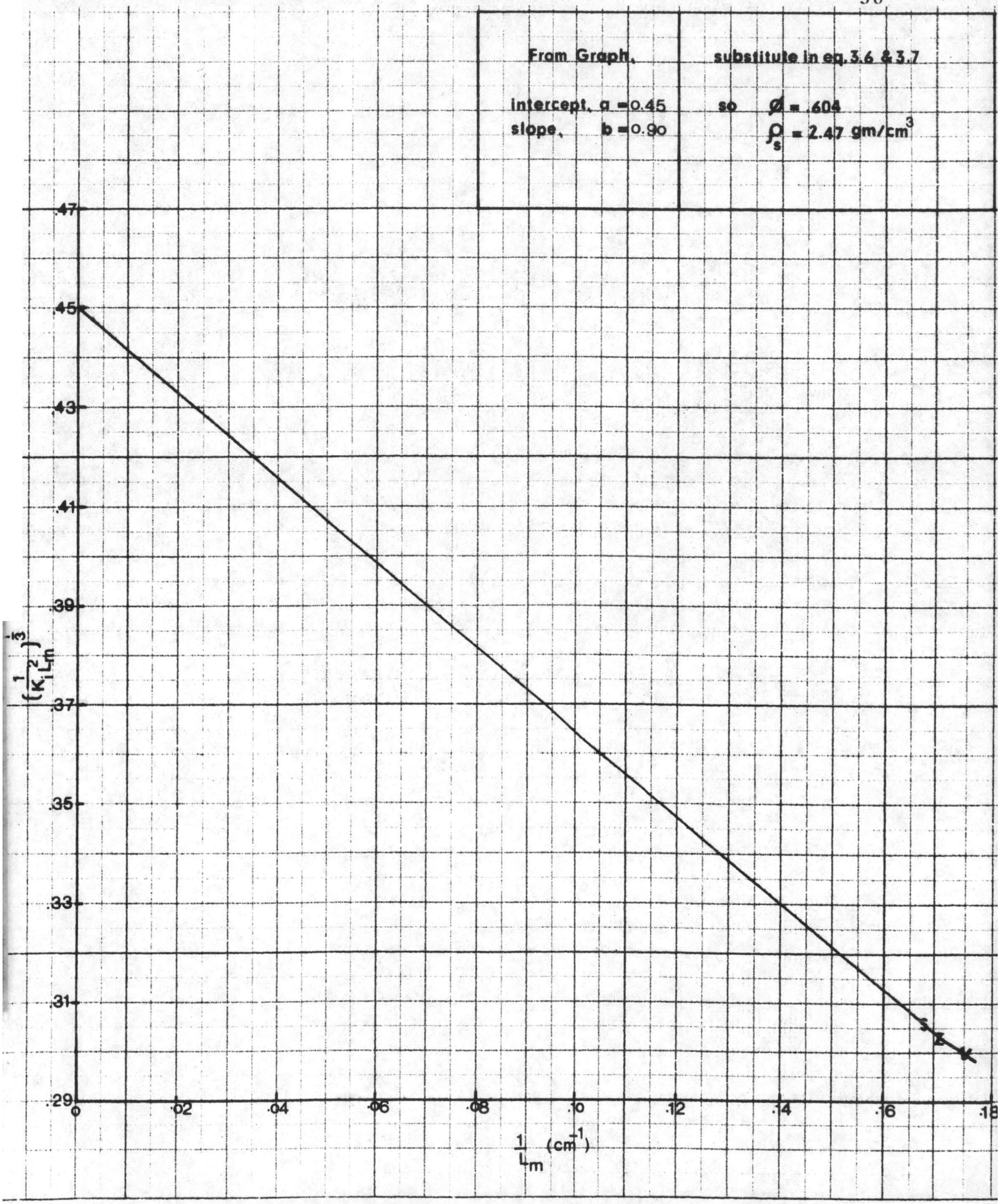

FIG. 4.2 – DETERMINATION OF ø & ρ_s IN EQ. (3-6) & EQ. (3-7)

FROM TABLE 4.2

and 3 were 36.00, 20.56, and 9.80 cm/sec., as shown in Fig. 4.3, 4.4, and 4.5, respectively. These minimum fluidizing velocities of each particle size were applied in fluidized bed retorting.

When spent shale particles, obtained from oil shale retorting at 550°C, were used instead of raw shale, the data of the actual minimum fluidizing velocities were tabulated in Table 4.4. For spent shale of the mean particle size of 0.680, 0.542, and 0.214 mm referred to as sample 1, 2, and 3, the velocities were 26.70, 14.16, and 7.15 cm/sec, respectively (Fig. 4.3 to 4.5). Thus the value of minimum fluidizing velocity of spent shale particles is lower than that of the raw shale by approximately 70% of minimum fluidizing velocity of raw shale. Besides, all the curves of spent shale shows that, when spent shale was operated at minimum fluidizing velocity for raw shale, there was no elutriation of the spent shale particles.

Table 4.3 Determination of U_{mf} for Raw Shale Particles

Run No.	Sample No.	W (gm)	$\bar{d}_p$ (mm)	U_o (cm/sec)	ΔP (mm.H_2O)	L_m (cm)
				0	0	5.80
				1.87	2.5	5.80
				3.93	4.4	5.80
				6.08	6.9	5.80
				10.47	13.3	5.80
				15.37	20.0	5.80
				23.37	29.0	5.80
1	1	100.00	0.715	29.44	35.0	5.80
				34.57	36.5	5.82
				35.96	37.0	5.86
				39.71	37.5	6.06
				45.00	37.5	6.65
				50.10	38.5	7.20
				59.98	39.0	8.50
				0	0	5.70
				1.87	4.1	5.70
				3.93	8.0	5.70
				6.08	12.0	5.70
				8.23	16.0	5.70
2	2	100.00	0.576	10.47	20.0	5.70

Table 4.3 (continued)

Run No.	Sample No.	W (gm)	$\bar{d}_p$ (mm)	U_o (cm/sec)	ΔP (mm.H_2O)	L_m (cm)
(2)	(2)	(100.00)	(0.576)	12.90	24.5	5.70
				15.37	29.5	5.70
				17.85	32.0	5.71
				20.56	35.8	5.75
				23.37	34.8	5.89
				26.17	35.0	6.31
				29.44	35.0	6.80
				32.72	35.5	7.50
				34.57	35.8	8.50
				0	0	6.00
				1.87	8.2	6.00
				6.08	26.0	6.00
				7.16	31.0	6.00
				8.23	32.5	6.15
				9.35	33.5	6.20
3	3	100.00	0.249	10.47	33.5	6.30
				12.90	33.7	6.40
				15.38	34.5	6.70
				20.56	36.0	7.20
				26.17	37.5	8.50

Note : Experiment at Room Temperature about 30°C.

Table 4.4 Determination of U_{mf} for Spent Shale Particles

Run No.	Sample No.	W (gm)	$\bar{d}_p$ (mm)	U_o (cm/sec)	ΔP (mm.H_2O)	L_m (cm)	Remarks
				0	0	5.49	Spent
				1.87	2.23	5.49	Shale
				3.93	4.30	5.49	of 100-
				6.08	6.50	5.49	gm Raw
				10.47	11.70	5.49	Shale
				15.37	16.60	5.49	Sample
				23.37	26.50	5.51	No. 1
1	1	77.24	0.680	26.17	28.00	5.53	
				29.44	27.80	5.57	
				34.57	28.05	5.70	
				37.81	28.30	6.20	
				39.71	28.50	8.15	
				50.10	29.50	8.45	
				59.98	30.50	8.90	
				0	0	5.40	Spent
				1.87	3.0	5.40	Shale
				3.93	7.4	5.40	of 100-
				8.23	16.6	5.40	gm Raw
				10.47	21.0	5.40	Shale
				11.73	23.0	5.43	Sample
2	2	76.98	0.542	12.90	25.93	5.45	No. 2
				14.16	26.25	5.50	
				15.38	26.27	5.60	
				16.64	26.19	5.70	
				17.84	26.20	5.80	
				20.56	26.71	6.20	

Table 4.4 (continued)

Run No.	Sample No.	W (gm)	$\bar{d}_p$ (mm)	U_o (cm/sec)	ΔP (mm.H_2O)	L_m (cm)	Remarks
(2)	(2)	(76.98)	(0.542)	23.34	26.90	6.50	
				29.44	28.00	8.00	
				38.51	29.10	8.80	
				0	0	5.50	Spent
				1.87	7.8	5.50	Shale
				3.93	15.0	5.50	of 100-
				6.08	23.7	5.50	gm Raw
				6.65	26.4	5.51	Shale
				7.16	27.0	5.53	Sample
3	3	77.32	0.214	8.23	26.2	5.57	No. 3
				9.35	27.0	5.70	
				10.47	27.1	6.00	
				12.90	27.8	6.45	
				15.38	28.5	7.20	
				20.56	30.0	8.00	
				26.17	31.0	8.50	

Note : Experiment at Room Temperature about 30 °C.

∀, .715 mm. Oil Shale Particle

S, .680mm. Spent Shale Particle

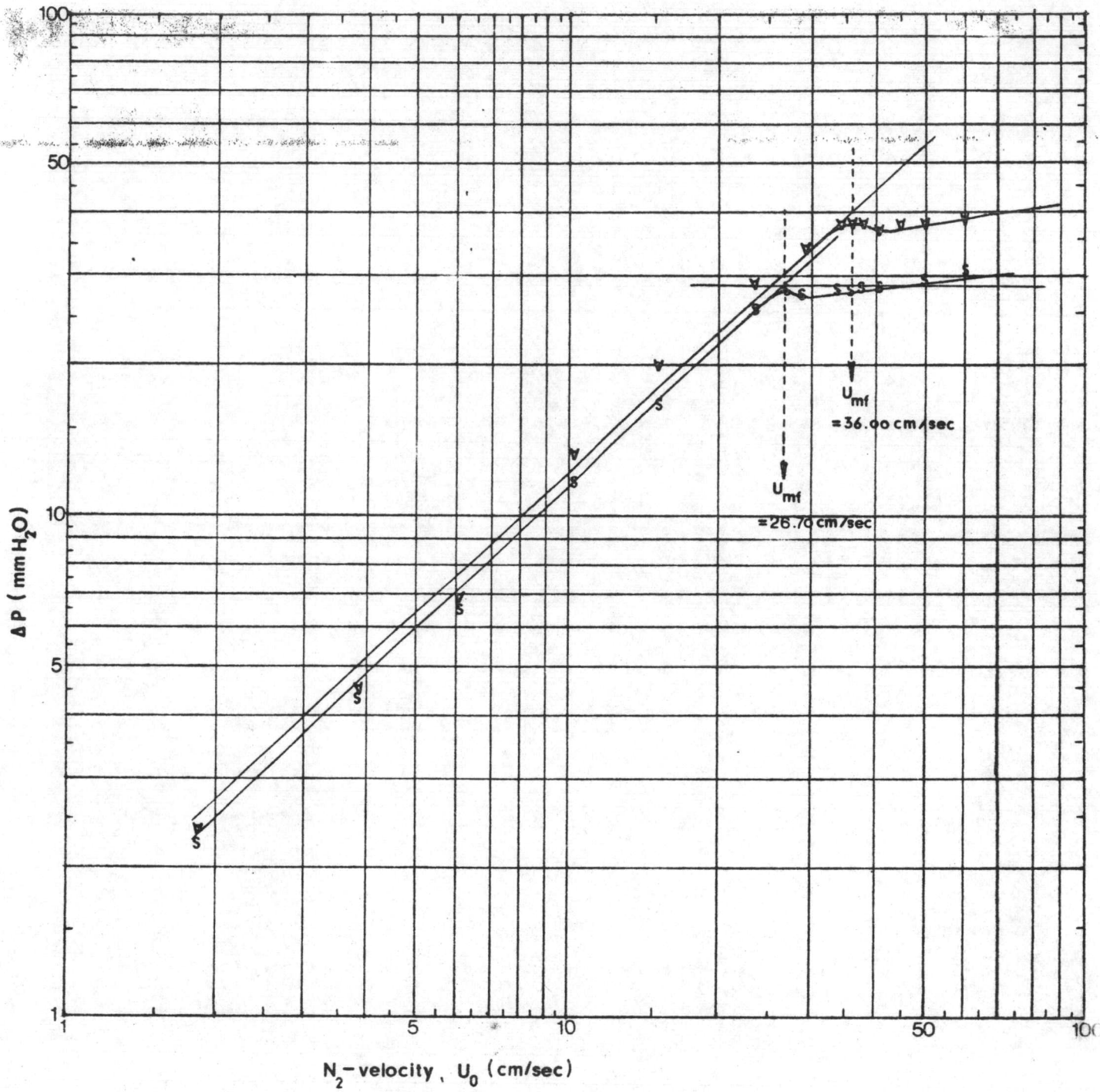

FIG. 4.3 – DETERMINATION OF U_{mf} ,

SAMPLE No. 1

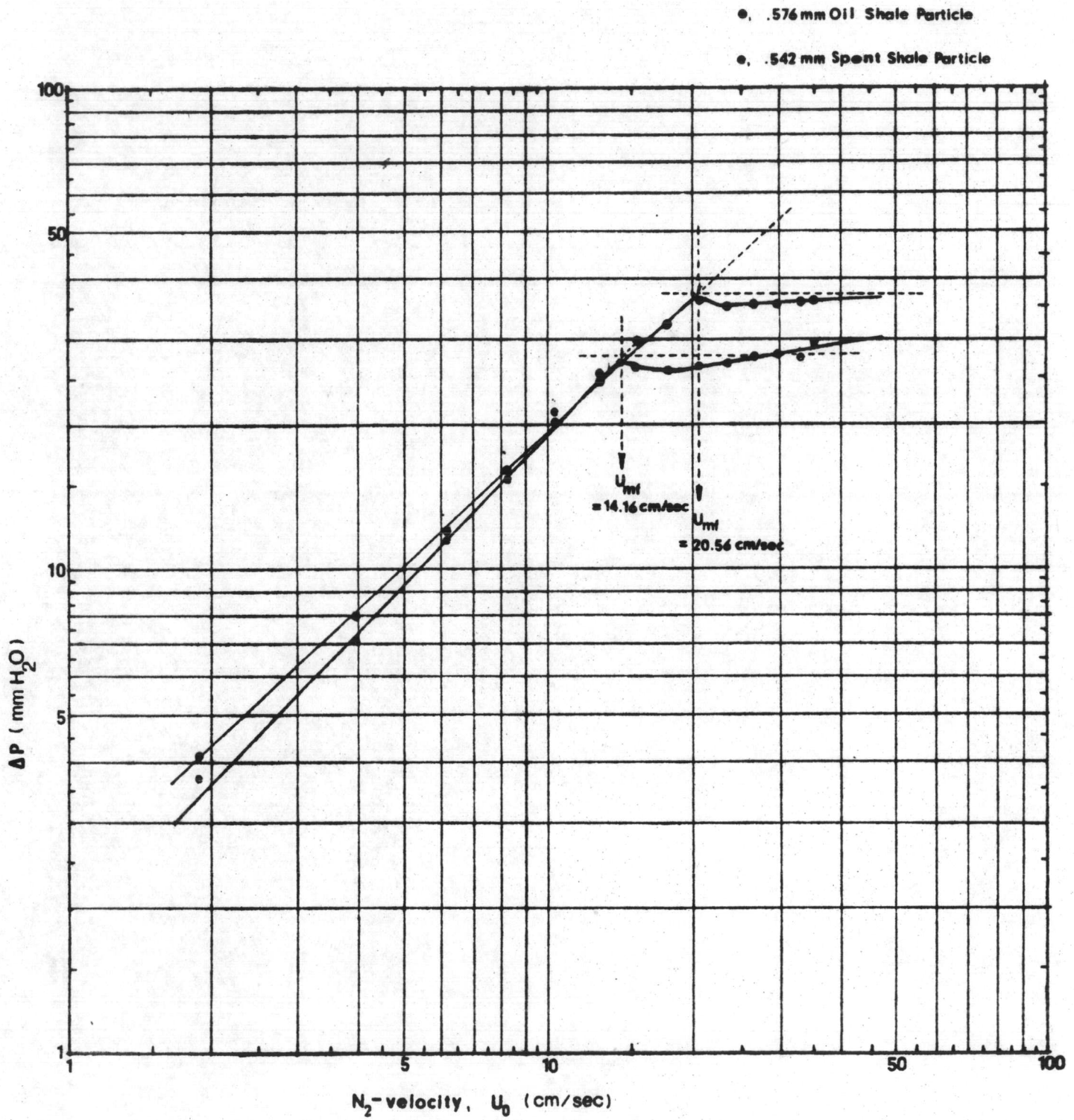

FIG. 4.4 - DETERMINATION OF U_{mf},

SAMPLE No. 2

●, .249 mm Oil Shale Particle

∀, .214 mm Spent Shale Particle

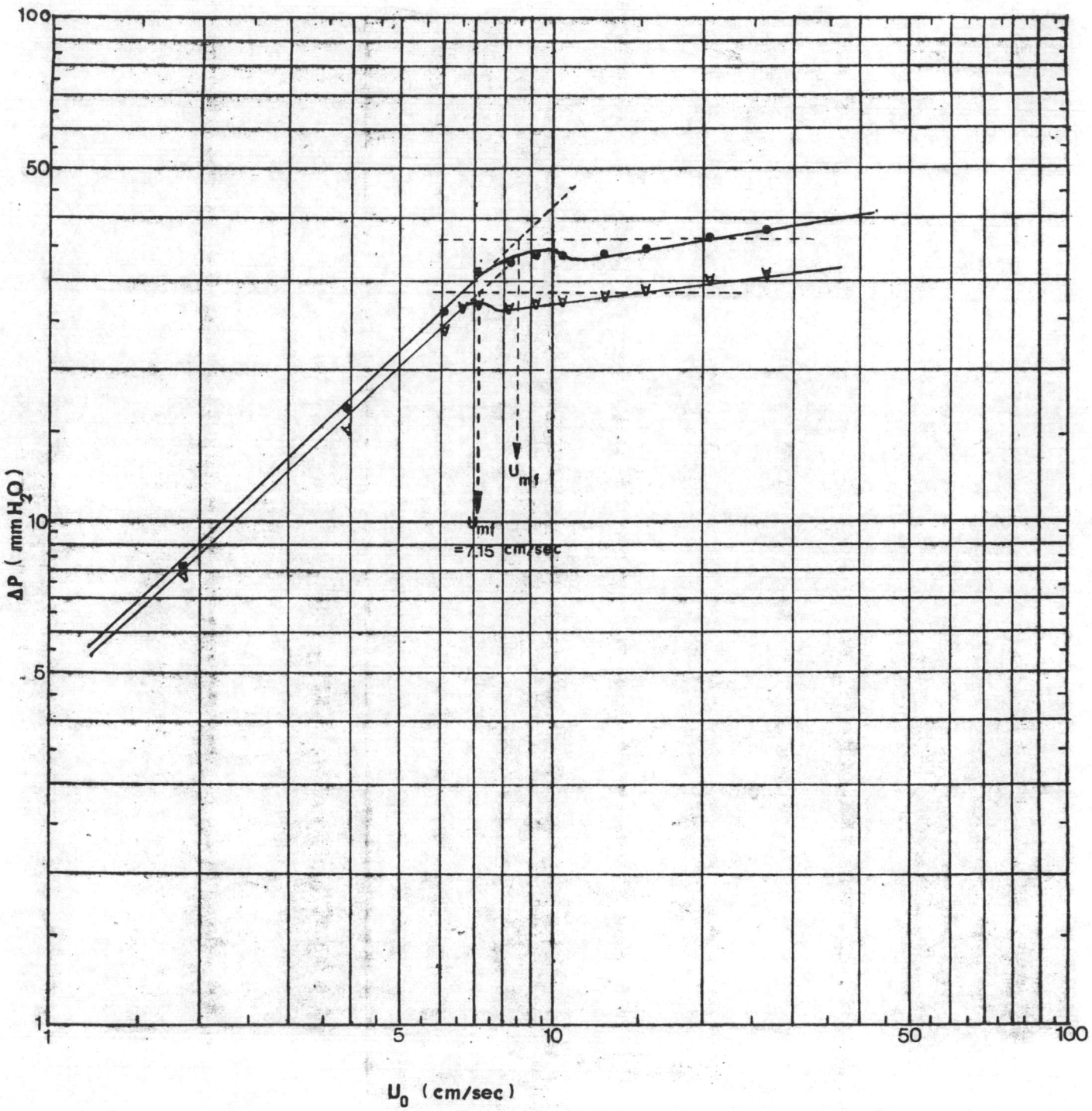

FIG. 4.5 – DETERMINATION OF U_{mf},

SAMPLE No. 3

4.3 The Effect of Retorting Temperature and Particle Size on Oil Yield

Oil shale, as analyzed by Fischer assay method, comprised of 11.69% oil, 4.15% water, 82.62% spent shale, and 1.54% gas and losses (Appendix B.5)

Table 4.5 and Fig. 4.6-A shows the effect of retorting temperature on oil yield of three different samples. The optimum temperature of sample 1,2, and 3 were 550, 560, and 580° C, with oil yield of 90.71, 107.05, and 106.37% by weight of Fischer assay, respectively. The result shows that the variation of the size of oil shale particles approximately did not effect the optimum temperature, as shown by the curve plotting between oil shale particle size and optimum temperature in Fig. 4.6-B. Therefore, the optimum temperature for the fluidized-bed retort would be 550-580°C.

The effect of particle size on oil yield is shown in Table 4.6 and Fig. 4.7. This was carried out at various retorting temperatures. 400, 450, 600, and 650°C. At the retorting temperatures of 400 and 450°C, the oil yield was nearly constant. At higher temperatures, 600 and 650°C, the oil yield decreased with increasing particle size. From the curve of retorting temperature of 550°C, it shows that maximum yield may be obtained at mean particle sizes of about 0.500-0.576 mm. The maximum oil yield is 107.05 wt % of Fischer assay.

Table 4.5 Effect of Retorting Temperature on Oil Yield.

W = 100.00 gm

U_{mf} at operating temperature was calibrated from Appendix B.4

Operating time 30 minutes (Appendix A.3 and A.4)

Oil content from Fischer assay = 11.69% (Appendix B.5)

Sample No.	Run No.	Retorting Temperature (°C)	Weight percent of products				Oil Yield (wt % F.A.)
			Oil	Water	Spent Shale	Gas and Losses	
1	1	400	9.68	2.00	79.45	8.87	82.84
	2	450	9.76	3.70	80.14	6.40	83.52
	3	500	9.90	2.70	78.98	8.42	84.72
	4	550	10.60	3.00	77.24	9.16	90.71
	5	600	9.68	2.15	74.28	13.89	82.84
	6	650	9.52	3.05	72.81	14.62	81.47
2	1	400	9.56	2.20	80.56	7.68	81.81
	2	450	10.10	2.50	79.80	7.60	86.43
	3	500	10.79	2.45	79.20	7.56	92.34
	4	550	12.51	2.37	76.98	8.14	107.05
	5	600	11.66	2.45	72.00	13.89	99.78
	6	650	9.77	2.60	70.00	17.63	83.61

Table 4.5 (continued)

Sample No.	Run No.	Retorting Temperature (°C)	Weight percent of products				Oil Yield (wt % F.A.)
			Oil	Water	Spent Shale	Gas and Losses	
	1	400	9.16	2.40	81.51	6.93	78.38
	2	450	9.95	1.50	79.20	9.35	85.15
	3	500	11.40	2.10	78.89	7.61	97.56
3	4	550	11.71	3.00	77.32	7.97	100.21
	5	600	12.43	2.60	73.19	11.78	106.37
	6	650	10.58	3.70	71.55	14.17	90.54

Note : wt % F.A. oil yield = $\frac{\text{wt \% in retorting of oil}}{\text{wt \% from Fischer assay of oil}} \times 100$

s Sample No. 1

∀ Sample No. 2

z Sample No. 3

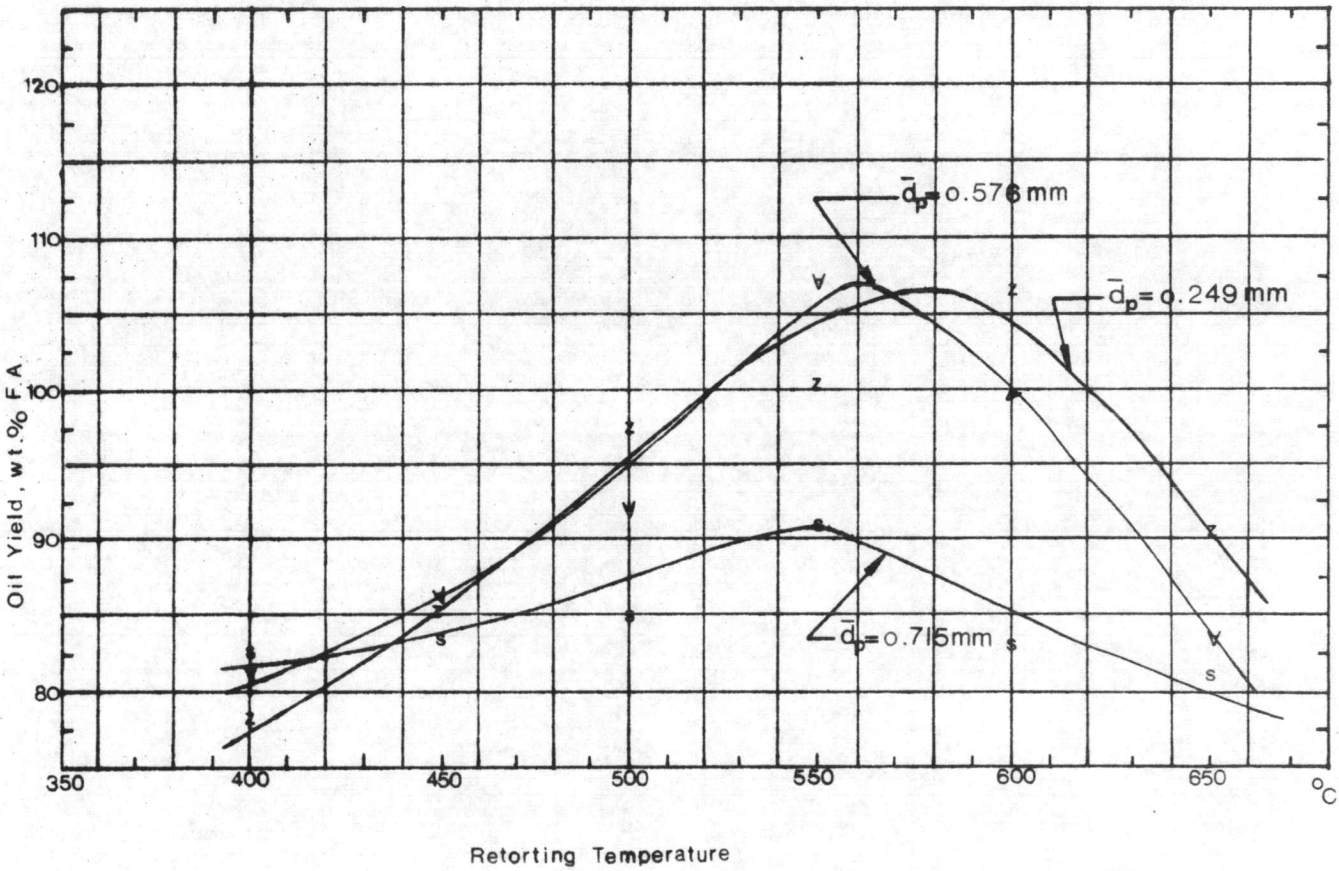

FIG. 4.6-A - EFFECT OF RETORTING TEMP.

ON OIL YIELD

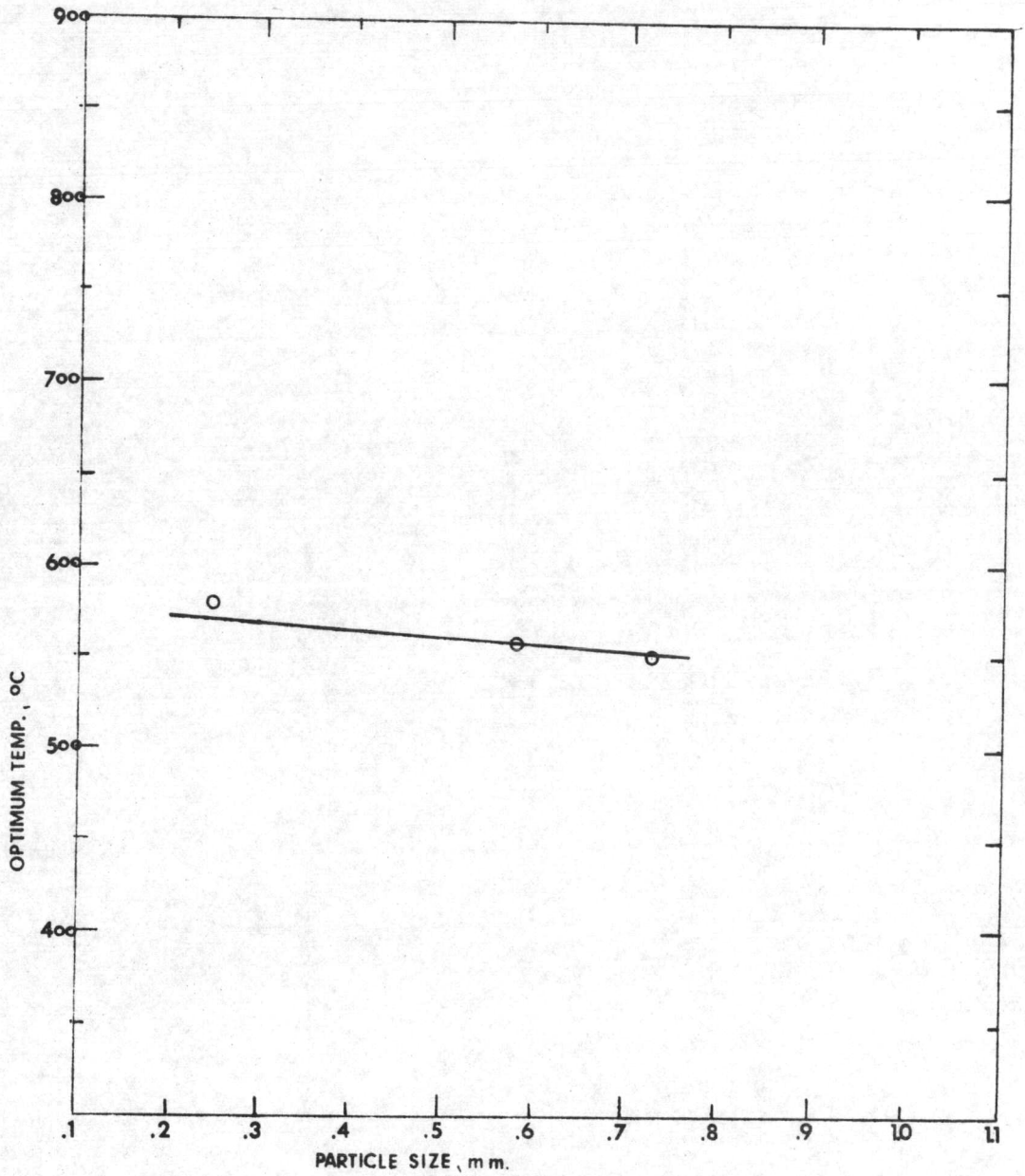

FIG. 4.6-B – CORRELATION OF OPTIMUM TEMPERATURE & PARTICLE SIZE OF OIL SHALE FROM FIG. 4.6-A.

Table 4.6 Effect of Particle Size on Oil Yield

Run No.	Retorting Temperature (°C)	$\bar{d}_p$ (mm)	wt % of products				Oil Yield (wt % F.A.)
			Oil	Water	Spent Shale	Gas and Losses	
1	400	0.249	9.16	2.40	81.51	6.93	78.38
2		0.576	9.56	2.20	80.56	7.68	81.81
3		0.715	9.68	2.00	79.45	8.87	82.84
1	450	0.249	9.95	1.50	79.20	9.35	85.15
2		0.576	10.10	2.50	79.80	7.60	76.43
3		0.715	9.76	3.70	80.14	6.40	83.52
1	500	0.249	11.40	2.10	78.89	7.61	97.56
2		0.576	10.79	2.45	79.20	7.56	92.34
3		0.715	9.90	2.70	78.98	8.42	84.72
1	550	0.249	11.71	3.00	77.32	7.97	100.21
2		0.576	12.51	2.37	76.98	8.14	107.05
3		0.715	10.60	3.00	77.20	9.16	90.71
1	600	0.249	12.43	2.60	73.19	11.78	106.37
2		0.576	11.66	2.45	72.00	13.89	99.78
3		0.715	9.68	2.15	74.28	13.89	82.84
1	650	0.249	10.58	3.70	71.55	14.17	90.54
2		0.576	9.77	2.60	70.00	17.63	83.61
3		0.715	9.52	3.05	72.81	14.62	81.47

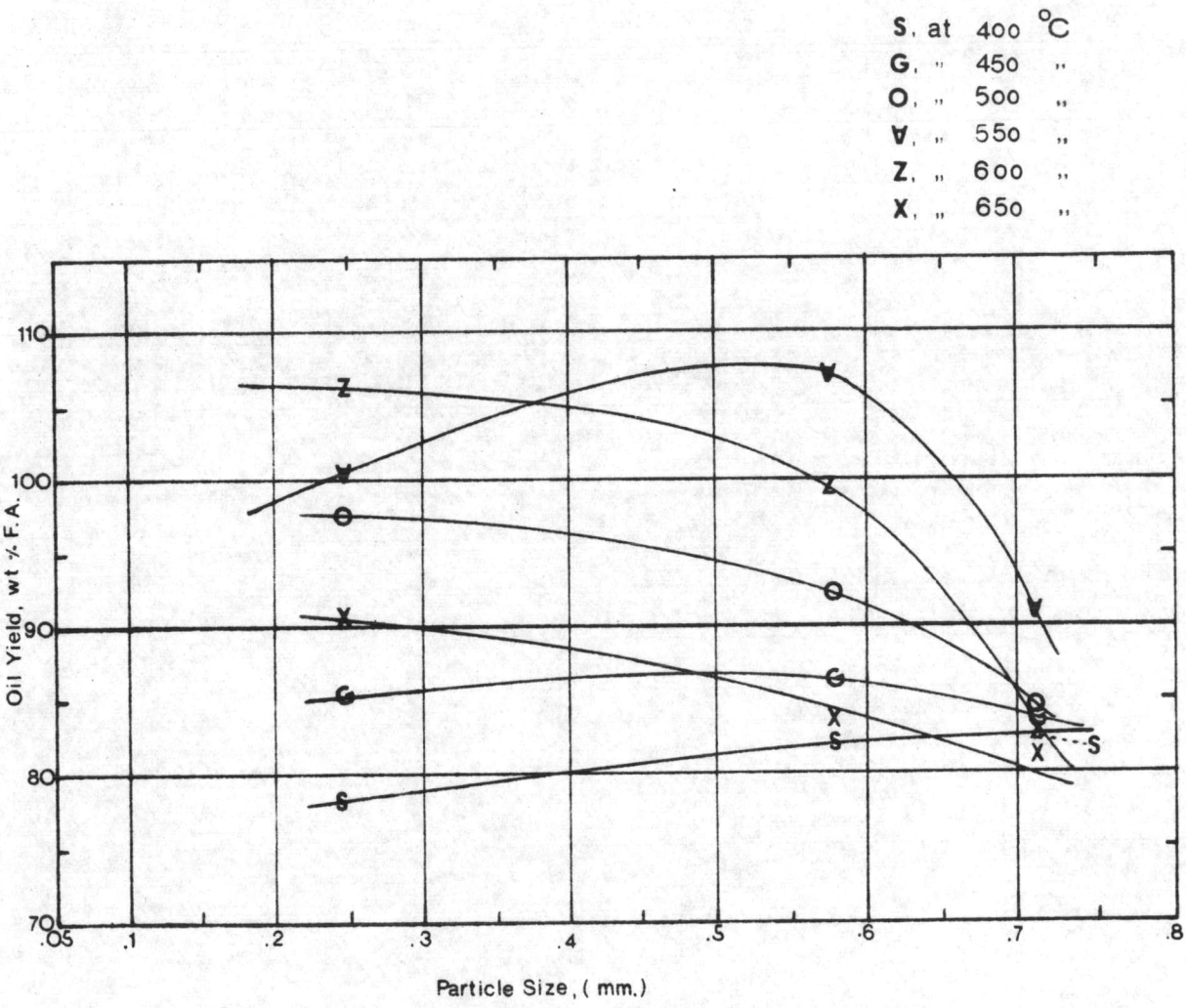

FIG. 4.7 - EFFECT OF PARTICLE SIZE ON OIL YIELD